THE JOURNAL OF BIOLOGICAL CHEMISTRY VOL. 290, NO. 42, pp. 25382–25394, October 16, 2015

Altered Lipid Synthesis by Lack of Yeast Pah1 Phosphatidate Phosphatase Reduces Chronological Life Span*

Received for publication, July 21, 2015, and in revised form, August 24, 2015 Published, JBC Papers in Press, September 3, 2015, DOI 10.1074/jbc.M115.680314

Yeonhee Park[‡], **Gil-Soo Han**[‡], **Eugenia Mileykovskaya**[§], **Teresa A. Garrett**[¶], **and George M. Carman**[‡1]

From the [‡]*Department of Food Science and the Rutgers Center for Lipid Research, New Jersey Institute for Food, Nutrition, and Health, Rutgers University, New Brunswick, New Jersey 08901, the* [§]*Department of Biochemistry and Molecular Biology, University of Texas-Houston Medical School, Houston, Texas 77030, and the* [¶]*Department of Chemistry, Vassar College, Poughkeepsie, New York 12604*

Background: Pah1 phosphatidate phosphatase regulates the synthesis of triacylglycerol and membrane phospholipids.
Results: The lack of Pah1 causes increases in phospholipid synthesis, ATP consumption, and oxidative stress and a decrease in chronological life span.
Conclusion: Pah1 plays a role in chronological life span by regulating lipid synthesis.
Significance: Pah1-mediated regulation of triacylglycerol and phospholipid syntheses is important for chronological life span.

In *Saccharomyces cerevisiae*, Pah1 phosphatidate phosphatase, which catalyzes the dephosphorylation of phosphatidate to yield diacylglycerol, plays a crucial role in the synthesis of the storage lipid triacylglycerol. This evolutionarily conserved enzyme also plays a negative regulatory role in controlling *de novo* membrane phospholipid synthesis through its consumption of phosphatidate. We found that the *pah1*Δ mutant was defective in the utilization of non-fermentable carbon sources but not in oxidative phosphorylation; the mutant did not exhibit major changes in oxygen consumption rate, mitochondrial membrane potential, F_1F_0-ATP synthase activity, or gross mitochondrial morphology. The *pah1*Δ mutant contained an almost normal complement of major mitochondrial phospholipids with some alterations in molecular species. Although oxidative phosphorylation was not compromised in the *pah1*Δ mutant, the cellular levels of ATP in quiescent cells were reduced by 2-fold, inversely correlating with a 4-fold increase in membrane phospholipids. In addition, the quiescent *pah1*Δ mutant cells had 3-fold higher levels of mitochondrial superoxide and cellular lipid hydroperoxides, had reduced activities of superoxide dismutase 2 and catalase, and were hypersensitive to hydrogen peroxide. Consequently, the *pah1*Δ mutant had a shortened chronological life span. In addition, the loss of Tsa1 thioredoxin peroxidase caused a synthetic growth defect with the *pah1*Δ mutation. The shortened chronological life span of the *pah1*Δ mutant along with its growth defect on non-fermentable carbon sources and hypersensitivity to hydrogen peroxide was suppressed by the loss of Dgk1 diacylglycerol kinase, indicating that the underpinning of *pah1*Δ mutant defects was the excess synthesis of membrane phospholipids.

The synthesis of lipids is an energy-consuming process that cells engage in throughout their growth (1–3). In logarithmically growing yeast,[2] a diverse set of membrane lipids (*e.g.* PS[3] and its derivatives PE and PC, PI and its derivatives phosphoinositides and sphingolipids, and phosphatidylglycerophosphate and its derivatives PG and CL) are synthesized from the precursor PA via the liponucleotide intermediate CDP-DAG (Fig. 1) (2, 3). As cells exhaust nutrients and progress into the stationary phase (*e.g.* quiescence), PA is channeled to DAG for the synthesis of TAG (Fig. 1) (4–6). Under certain growth conditions (*e.g.* supplementation with choline or ethanolamine), the DAG derived from PA is also used for the synthesis of PC or PE by way of the CDP-choline or CDP-ethanolamine branches, respectively, of the Kennedy pathway (Fig. 1) (3). Quiescent cells may resume logarithmic growth if supplemented with fresh medium, and the TAG synthesized during the transition to stationary phase is mobilized to DAG and free fatty acid that are converted back to PA for conversion to CDP-DAG and the synthesis of membrane phospholipids (Fig. 1) (2, 3, 7–10).

The partitioning of PA to CDP-DAG and DAG in yeast is largely controlled by Pah1 PAP (11), a peripheral membrane-associated enzyme that catalyzes the Mg^{2+}-dependent dephosphorylation of PA to produce DAG (2, 3, 12–14). Pah1 PAP activity is relatively low in logarithmically growing cells, whereas the activity is induced as cells progress into the stationary phase (6). Pah1 PAP activity is regulated on multiple levels to control lipid metabolism. The expression of *PAH1* is controlled by growth phase and nutrient status (6, 15), and the catalytic efficiency of Pah1 PAP is controlled by membrane lipids (16, 17), nucleotides (18), and by its phosphorylation and dephosphorylation (19–22). The phosphorylation status of the enzyme also controls its association with the membrane (19, 20, 23–25) as well as its abundance through proteasomal degradation (26–28).

* This work was supported, in whole or in part, by National Institutes of Health Grant GM028140 (to G. M. C.) from the USPHS. This work was also supported by National Science Foundation Major Research Instrumentation Award 1039659 (to T. A. G). The authors declare that they have no conflicts of interest with the contents of this article.
[1] To whom correspondence should be addressed: Dept. of Food Science, Rutgers University, 65 Dudley Rd., New Brunswick, NJ 08901. Tel.: 848-932-5407; E-mail: carman@aesop.rutgers.edu.

[2] In this paper, the term yeast is used interchangeably with *S. cerevisiae*.
[3] The abbreviations used are: PS, phosphatidylserine; PAP, phosphatidate phosphatase; PA, phosphatidate; DAG, diacylglycerol; TAG, triacylglycerol; PC, phosphatidylcholine; PE, phosphatidylethanolamine; PI, phosphatidylinositol; CL, cardiolipin; ER, endoplasmic reticulum.

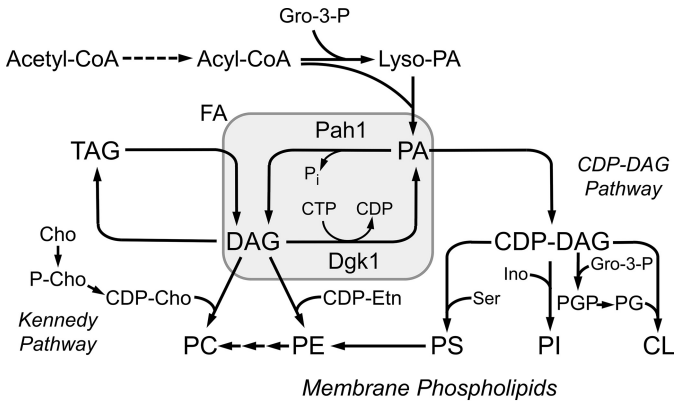

FIGURE 1. **Lipid synthesis in *S. cerevisiae*.** The pathways shown in the figure include the relevant steps discussed in this work. The PAP reaction catalyzed by Pah1 is found at the branch point in lipid synthesis where PA is converted to DAG or CDP-DAG for the synthesis of TAG or membrane phospholipids, respectively. The PAP reaction is counterbalanced by the DAG kinase reaction catalyzed by Dgk1, and together, these enzyme reactions (highlighted by *gray shading*) play a major role in controlling the balance of PA and DAG. The *dashed arrow* leading from acetyl-CoA to acyl-CoA represents the many steps needed to form the fatty acyl moieties of lipids. The early steps for PE synthesis in the CDP-ethanolamine branch of the Kennedy pathway and the CL remodeling steps are not shown in the figure. A more detailed map of lipid synthesis pathways that also include the PI-derived synthesis of polyphosphoinositides and complex sphingolipids may be found elsewhere (3). *Gro-3-P,* glycerol-3-phosphate; *FA,* fatty acid; *Cho,* choline; *P-Cho,* phosphocholine; *Etn,* ethanolamine; *Ino,* inositol; *PGP,* phosphatidylglycerophosphate.

PAP activity is governed by the D*X*D*X*T catalytic motif within a haloacid dehalogenase-like domain in Pah1 that is conserved in mammalian lipin PAP enzymes (11, 29, 30). Genetic and biochemical studies of Pah1 and its mammalian orthologs (*i.e.* lipins) have revealed that the PAP enzyme is a major regulator of lipid homeostasis and cell physiology (12–14, 31–33). The importance of Pah1 in lipid metabolism is indicated by diverse phenotypes of the *pah1*Δ mutant, many of which are related to the increased level of PA and the decreased levels of DAG and TAG (11, 29, 34–36). The increased level of PA induces the expression of UAS_{INO}-containing phospholipid synthesis genes and an increase in membrane phospholipid synthesis (6, 11, 34, 35, 37). Considering that PAP activity is elevated as yeast cells progress to the stationary phase (6), the effect of the enzyme loss on phospholipid synthesis is greater in the stationary phase than in the exponential phase (6, 11, 35). The increased levels of phospholipids in the *pah1*Δ mutant are presumably responsible for its aberrant expansion of the nuclear/ER membrane (29, 34). The reduced levels of DAG and TAG in the *pah1*Δ mutant correlate with a reduced number of lipid droplets (35, 36), and the inability to synthesize TAG results in the accumulation of fatty acids giving rise to growth sensitivity to palmitoleic and oleic acids (35).

The *pah1*Δ mutant also exhibits phenotypes whose molecular basis in connection with its altered lipid metabolism is not yet clear. It is defective in vacuole fusion and exhibits small fragmented vacuoles as opposed to a large vacuole in the stationary phase (38). Cells lacking Pah1 are defective in cell wall integrity and easily ruptured by sonication (39, 40). In addition, the *pah1*Δ mutant exhibits a high mannose-to-glucose ratio, a high level of *N*-acetylglucosamine, and is hypersensitive to K1 killer toxin (39). Moreover, *pah1*Δ mutant cells are temperature-sensitive (11, 34, 41), are unable to grow on glycerol, a non-fermentable carbon source (11, 41), and exhibit apoptotic and necrotic phenotypes (35). The inability to grow on glycerol has suggested that *pah1*Δ mutant cells are respiratory-deficient (41). In this work, we confirmed that the mutant is defective in growth on glycerol and other non-fermentable carbon sources, but this phenotype was ascribed to reduced levels of ATP through its overconsumption for lipid synthesis rather than due to a defect in oxidative phosphorylation. Moreover, the *pah1*Δ mutant was susceptible to oxidative stress, which together with reduced ATP contributed to a shortened chronological life span. These phenotypes of the *pah1*Δ mutant were partially complemented by loss of the Dgk1 DAG kinase, indicating that an underlying mechanism is the excess synthesis of membrane phospholipids.

Experimental Procedures

Materials—All chemicals were reagent grade or better. Growth medium components were obtained from Difco Laboratories. BacTiter-Glo™ microbial cell viability assay kit was purchased from Promega. Phusion high fidelity DNA polymerase and the DNA gel extraction kit were purchased from New England Biolabs and Qiagen, respectively. Carrier DNA for yeast transformation was from Clontech. DNA size ladders, molecular mass protein standards, electrophoresis reagents, Triton X-100, Bio-Safe Coomassie G-250, and protein assay reagents were from Bio-Rad. PVDF membrane and the enhanced chemifluorescence Western blotting substrate were from GE Healthcare. Life Technologies, Inc., was the source of mouse anti-porin, anti-carboxypeptidase Y, anti-OxPhos antibody against subunit III of complex IV and anti-phosphoglycerate kinase antibodies and the source of MitoSOX™ Red mitochondrial superoxide indicator, tetramethylrhodamine methyl ester, and 3–12% polyacrylamide gradient gels. Alkaline phosphatase-conjugated goat anti-mouse IgG antibodies and goat anti-rabbit IgG antibodies were from Pierce and Thermo Scientific, respectively. Aprotinin, ATP, benzamidine, bovine serum albumin, DTT, hydrogen peroxide, leupeptin, lyticase, pepstatin, PMSF, sodium azide, and xylenol orange were purchased from Sigma. Radiochemicals and primulin were from PerkinElmer Life Sciences and MP Biomedicals, respectively. Acrylamide solutions and scintillation counting supplies were from National Diagnostics. Silica gel 60 and LK5D TLC plates were obtained from EM Science and Whatman, respectively. Lipids were obtained from Avanti Polar Lipids with the exception of heptadecanoic acid, which was from Alfa Aesar.

Strains and Growth Conditions—The yeast strains used in this study are listed in Table 1. Standard methods were used for culturing yeast (42, 43). Cells were grown at 30 °C in synthetic complete (SC) medium, which contained 2% glucose as the carbon source, YPD (1% yeast extract, 2% peptone, 2% glucose) medium or YPEG (1% yeast extract, 2% peptone, 0.95% ethanol, 3% glycerol) medium. The ethanol in YPEG medium allows for growth of *pah1*Δ, which otherwise does not occur in medium with glycerol as the sole carbon source. Where indicated, glucose was replaced in SC or YPD media with 2% ethanol, 3% glycerol, 2% acetate, or 2% lactate. Growth of cells in liquid medium was measured spectrophotometrically at $A_{600\,nm}$. For measurement of growth on solid medium, liquid cultures were

TABLE 1
Strains and plasmids used in this study

Strain or plasmid	Genotype or relevant characteristics	Source or Ref.
E. coli		
DH5α	F$^-$ ϕ80d*lacZ*ΔM15Δ (*lacZYA-argF*)U169 *deoR recA*1 *endA*1 *hsdR*17 (r_k^- m_k^+) *pho*A *sup*E44 λ$^-$ *thi*-1 *gyr*A96 *rel*A1	42
S. cerevisiae		
W303-1A	*MAT***a** *ade2-1 can1-100 his3-11,15 leu2-3,112 trp1-1 ura3-1*	120
GHY57	*pah1*Δ::*URA3* derivative of W303-1A	11
YPY3	*dgk1*Δ::*HIS3* derivative of W303-1A	This study
YPY4	*dgk1*Δ::*HIS3 pah1*Δ::*URA3* derivative of W303-1A	This study
YPY5	*tsa1*Δ::*kanMX4* derivative of W303-1A	This study
YPY6	*pah1*Δ::*URA3 tsa1*Δ::*kanMX4* derivative of W303-1A	This study
Plasmid		
pGH317	*pah1*Δ::*URA3* inserted into YEp351	11
pYX142-mtGFP	Plasmid for the expression of the mitochondria target GFP	53

adjusted to $A_{600\ nm} = 0.67$, followed by 10-fold serial dilutions. The serially diluted cell suspensions were spotted onto solid medium, and growth was scored after incubation for 2–3 days. For the analysis of chronological life span (44), cultures in SC medium were diluted in fresh medium at $A_{600\ nm} = 0.01$ and grown to the exponential phase ($A_{600\ nm} = 1$). The exponential phase cells were diluted in fresh medium at $A_{600\ nm} = 0.1$ and grown for 2 days to the stationary phase. The stationary phase culture (day 0 in chronological life span experiments) was then incubated for 10 days during which aliquots were taken on a daily basis and plated onto YPD agar plates. Colonies formed after incubation for 2 days were counted as being produced from viable cells. The viability at day 0 was set at 100%.

DNA Manipulations and Construction of Mutants—The plasmids used in this study are listed in Table 1. Standard methods were used for isolation of chromosomal and plasmid DNA, for digestion and ligation of DNA, and for PCR amplification of DNA (42). Transformations of *Escherichia coli* (42) and yeast (45) were performed as described previously. Yeast deletion mutations were generated by the method of one-step gene replacement (46). For construction of the *dgk1*Δ mutant (YPY3), the parental strain W303-1A was transformed with the *dgk1*Δ::*HIS3* disruption cassette that was amplified by PCR from the genomic DNA of the *dgk1*Δ::*HIS3* mutant in the RS453 strain background (47). The yeast transformant exhibiting histidine prototrophy was confirmed for the deletion of *DGK1* by PCR analysis. For construction of the *dgk1*Δ *pah1*Δ mutant (YPY4), strain YPY3 was transformed with the *pah1*Δ::*URA3* disruption cassette that was released from pGH317 by digestion with XbaI and SphI (11). The *dgk1*Δ transformant exhibiting uracil prototrophy was confirmed for the deletion of *PAH1* by PCR analysis. For construction of the *tsa1*Δ mutant (YPY5), the parental strain W303-1A was transformed with the *tsa1*Δ::*kanMX4* disruption cassette that was amplified by PCR from the genomic DNA of *tsa1*Δ::*kanMX4* mutant in the BY4741 strain background (yeast deletion consortium). The *pah1*Δ *tsa1*Δ mutant strain YPY6 was constructed by transformation of the *pah1*Δ mutant strain GHY57 with the *tsa1*Δ::*kanMX4* disruption cassette. These *tsa1*Δ and *pah1*Δ *tsa1*Δ mutations were confirmed by PCR analysis and DNA sequencing.

Preparation of Cell Extracts—All steps to prepare cell extracts were performed at 4 °C. Yeast cultures were harvested at 1,500 × *g* for 5 min, washed with water, and resuspended in lysis buffer (50 mM Tris-HCl, pH 7.5, 0.3 M sucrose, 10 mM 2-mercaptoethanol, 0.5 mM PMSF, 1 mM benzamidine, 5 μg/ml aprotinin, 5 μg/ml leupeptin, and 5 μg/ml pepstatin). The cell suspension was added with glass beads (0.5-mm diameter) and then subjected to five repeats of a 1-min burst and a 2-min cooling using a BioSpec Products Mini-Beadbeater-16 (48). The disrupted cells were centrifuged at 1,500 × *g* for 10 min to separate unbroken cells and cell debris (pellet) from cell extracts (supernatant). The protein concentration was determined by the method of Bradford (49) using bovine serum albumin as a standard.

Isolation of Mitochondria and Analysis of Morphology—Mitochondria were isolated from disrupted spheroplasts by differential centrifugation followed by sucrose gradient centrifugation according to the procedures described by Meisinger *et al.* (50). Western blot analysis with anti-porin (mitochondrial marker), anti-carboxypeptidase Y (vacuole marker), anti-phosphatidylserine synthase (ER marker) (51), and anti-phosphoglycerate kinase (cytosol marker) antibodies showed that the mitochondrial preparations used in the study were highly purified and essentially devoid of contaminating fractions. Purified mitochondria were prepared for electron microscopy (52) and visualized using a JEOL 1200EX transmission electron microscope at 60 kV and captured with Gatan Orius 830 digital imaging system. Mitochondrial tubulation in cells expressing plasmid pYX142-mtGFP (53) was examined for fluorescence using a Zeiss LSM 710 confocal microscope.

PAGE and Western Blot Analysis—SDS-PAGE (54) using 10% slab gels and Western blotting (55, 56) using a PVDF membrane were performed as described previously. Primary mouse and rabbit antibodies were routinely used at a dilution of 1:1,000. Alkaline phosphatase-conjugated goat anti-mouse and anti-rabbit IgG antibodies were used at a dilution of 1:5,000. Immunecomplexesweredetectedusingtheenhancedchemifluorescence Western blotting substrate. Fluorimaging was used to acquire fluorescence signals from immunoblots, and the intensities of the images were analyzed using ImageQuant software. Blue native-PAGE (57) of digitonin-lysed mitochondria (58) was performed with a 3–12% linear gradient slab gel at 4 °C for 20 h. Following electrophoresis, the polyacrylamide gel was stained with Coomassie Blue or electroblotted onto a PVDF membrane. The protein complexes on the PVDF membrane were detected by immunoblotting with anti-OxPhos antibody against subunit III of complex IV (58). Data were analyzed with Quantity One software from Bio-Rad.

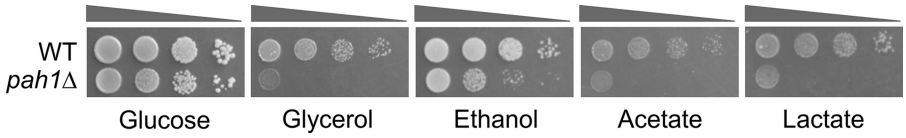

FIGURE 2. ***pah1*Δ mutant exhibits a growth defect on non-fermentable carbon sources.** Wild type and *pah1*Δ mutant cells were grown at 30 °C to saturation in YPD medium. The cultures were washed and resuspended in water at $A_{600\ nm} = 0.67$. After 10-fold serial dilutions, 5 μl of each cell suspension was spotted onto YP agar medium containing the indicated carbon source, followed by incubation for 3 days (2% glucose) or 5 days (2% ethanol, 2% acetate, 2% lactate, or 3% glycerol). The data are representative of three independent experiments.

Lipid Extraction and Analysis—Lipids were extracted from purified mitochondria by the method of Bligh and Dyer (59). Mitochondrial phospholipids were separated on silica gel plates by two-dimensional TLC (60). The separated lipids were stained with primulin (61), subjected to fluoroimaging, and quantified with ImageQuant software. The identity of phospholipids was confirmed by comparison with standards. The fatty acid composition of the mitochondrial lipids after deacylation was determined by gas-liquid chromatography (35) using heptadecanoic acid as an internal standard. The mitochondrial phospholipid molecular species were analyzed by liquid chromatography-electrospray ionization quadrupole time-of-flight mass spectrometry (62, 63). For radiolabeling of cellular neutral lipids and total phospholipids, cells were grown in SC medium to the late exponential phase ($A_{600\ nm}$ ~1). The cells were harvested, washed, and resuspended in SC medium with glycerol as the carbon source and [2-^{14}C]acetate (1 μCi/ml). After incubation for 2 or 4 h, the radiolabeled cells were harvested; the lipids were extracted (59) and separated by one-dimensional TLC on Silica Gel 60 plates (64). [2-^{14}C]Acetate was used as a standard to calculate the radioactivity of the radiolabeled lipids. For radiolabeling of phosphoinositol-containing sphingolipids, cells were grown to the stationary phase in SC medium containing *myo*-[2-^{3}H]inositol (10 μCi/ml). The lipids were extracted and deacylated, and the radiolabeled sphingolipids were separated by one-dimensional TLC on silica gel LK5D plates (65–67). The radiolabeled lipids on TLC plates were visualized by phosphorimaging and quantified with ImageQuant software.

Measurements of Oxygen Consumption, Mitochondrial Membrane Potential, ATP, Superoxides, and Lipid Hydroperoxides—Cells were diluted 10-fold in fresh medium and assayed for oxygen consumption using an oxygen electrode in a 500-μl chamber (68). Mitochondrial oxygen consumption was confirmed with controls that contained 0.05% sodium azide. Mitochondrial membrane potential was measured with tetramethylrhodamine methyl ester, a cationic red-orange fluorescent dye that is readily sequestered by active mitochondria. Cells were washed twice with phosphate-buffered saline, pH 7.0, and then incubated for 30 min at 30 °C in buffer containing 40 μM tetramethylrhodamine methyl ester. After washing with phosphate-buffered saline, 10^{4}-labeled cells were measured for fluorescence. ATP was measured with the BacTiter-Glo™ microbial cell viability assay kit. Cells were resuspended in 80 μl of sterile water and mixed with an equal volume of BacTiter-Glo™ reagent in 96-well opaque plates. After incubation for 3 min, the luminescence produced was measured. ATP (0.1–100 μM) was used as a standard in the assay. Superoxides were measured with MitoSOX Red, a mitochondrial superoxide indicator. Cells were washed twice with phosphate-buffered saline, pH 7.0, and incubated for 30 min at 30 °C in the buffer containing 5 μM MitoSOX Red. After washing twice with phosphate-buffered saline, 10^{4}-labeled cells were measured for fluorescence. Lipid hydroperoxides were measured by the ferrous oxidation-xylenol orange complex assay using hydrogen peroxide as a standard (69).

Enzyme Assays—Oligomycin-sensitive F_1F_0-ATP synthase activity was measured by following the reverse ATPase reaction using a coupled spectrophotometric assay (70, 71). The reaction mixture contained 50 mM HEPES-KOH, pH 8.0, 5 mM $MgSO_4$, 2.5 mM ATP, 2.5 mM phosphoenolpyruvate, 0.3 mM NADH, 2 μg/ml antimycin, 50 μg/ml pyruvate kinase, 50 μg/ml lactate dehydrogenase, and 20 μg of mitochondria with and without 2 μg/ml oligomycin. Sod1 and Sod2 superoxide dismutase activities were determined in polyacrylamide gels by nitro blue tetrazolium-negative staining (72, 73). Catalase activity was measured by following the decomposition of hydrogen peroxide at $A_{240\ nm}$ (74). The reaction mixture contained 50 mM potassium phosphate buffer, pH 7.0, 20 mM hydrogen peroxide, and 20 μg of cell extract. All enzyme assays were performed in triplicate and were linear with time and protein concentration. A unit of ATPase was defined as nanomoles/min and catalase was defined as micromoles/min.

Analyses of Data—Statistical analyses were performed with SigmaPlot software. The p values of <0.05 were taken as a significant difference.

Results

*pah1*Δ *Mutant Exhibits a Growth Defect on Non-fermentable Carbon Sources*—One of the distinct phenotypes shown by the *pah1*Δ mutant is the lack of growth on glycerol (11, 41). Because non-fermentable carbon sources are metabolized through mitochondrial respiration, the growth defect of the *pah1*Δ mutant has been attributed to respiratory deficiency (41). To further confirm this phenotype, we examined the growth of the *pah1*Δ mutant on acetate, ethanol, and lactate (Fig. 2). As on glycerol, the *pah1*Δ mutant did not show growth on acetate or lactate. Although the *pah1*Δ mutant grew on ethanol, its growth was much less than that of the wild type control.

*Morphology, Phospholipid Composition, and Supercomplex Formation in Mitochondria of the pah1*Δ *Mutant*—The growth defect of the *pah1*Δ mutant on non-fermentable carbon sources raised a question about its mitochondrial morphology and phospholipid composition. Accordingly, these attributes were examined with purified mitochondria. Electron microscopic analysis of the mitochondria purified from wild type and *pah1*Δ mutant cells grown in YPEG medium showed no major difference in morphology. The mitochondrial morphology of cells grown on YPEG or in SC medium was also examined by

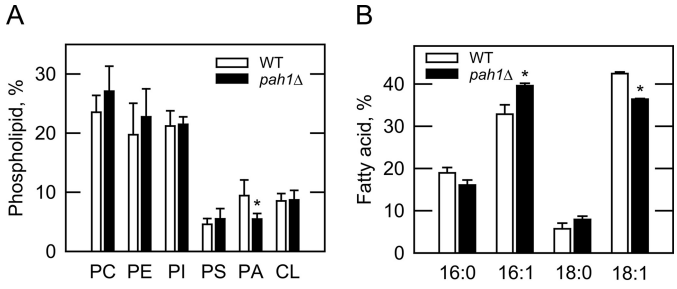

FIGURE 3. **Effects of the *pah1*Δ mutation on the compositions of phospholipids and fatty acids in the mitochondria.** Lipids were extracted from the mitochondria of wild type and *pah1*Δ mutant cells grown to the stationary phase in SC medium. *A*, phospholipids were separated by two-dimensional TLC, stained with 0.05% primulin, and then subjected to fluorimaging and ImageQuant analysis. *B*, lipids were subjected to transmethylation and analyzed by gas-liquid chromatography. The sum of the phospholipids that include unidentified signals or fatty acids in *A* or *B*, respectively, was set to 100%. Each data point represents the average of three experiments ± S.D. (*error bars*). *, $p < 0.05$ *versus* WT.

fluorescence microscopy using a mitochondrion-targeted GFP (53). In this analysis, the mitochondria of the *pah1*Δ mutant exhibited the tubulated morphology that is characteristic of stationary phase cells with mitochondrial function (53).

Mitochondrial phospholipids (*e.g.* CL and PE) play important roles in mitochondrial function that include electron transport, oxidative phosphorylation, and stabilization of the respiratory supercomplexes (58, 75–77). Accordingly, we examined the phospholipid composition of the mitochondria purified from *pah1*Δ cells grown to the stationary phase in SC medium. This analysis showed that the mass of mitochondrial lipids of the *pah1*Δ mutant (*e.g.* 221 ± 27 μg of lipid/mg of protein) was not significantly different from that of the wild type control (*e.g.* 233 ± 13 μg of lipid/mg of protein). The composition of the major phospholipids PC, PE, PI, and PS, as well as the mitochondrion-specific phospholipid CL, was not significantly affected by the *pah1*Δ mutation (Fig. 3*A*). However, the *pah1*Δ mutation caused the amount of PA to decrease by 42% (Fig. 3*A*). The amount of the minor mitochondrial phospholipid PG was too low for detection in this analysis. The fatty acid composition of total mitochondrial lipids was analyzed by gas-liquid chromatography. As described previously for whole cell extracts (35), the major fatty acyl species of the mitochondria of wild type and *pah1*Δ mutant cells were palmitic, palmitoleic, stearic, and oleic acids (Fig. 3*B*). The effects of the *pah1*Δ mutation were a relatively small (20%) increase in palmitoleic acid and a corresponding small decrease (15%) in oleic acid. The relative amounts of palmitic acid and steric acid were not significantly affected by the *pah1*Δ mutation.

The molecular species of the mitochondrial phospholipids were determined by liquid chromatography-electrospray ionization quadrupole time-of-flight mass spectrometry (Fig. 4). This analysis distinguishes the molecular species of a given phospholipid class that have different *m/z* values and thus identifies each by the total number of carbons and the degree of unsaturation in the acyl chains. By normalizing the mass of mitochondria prior to lipid extraction, we were able to examine differences in the individual phospholipid molecular species between the *pah1*Δ mutant and the wild type control. The major changes (*e.g.* ~2-fold) caused by the *pah1*Δ mutation in phospholipids with two fatty acyl chains were increases in species with 32 carbons (*e.g.* PE, PS, and PG) and decreases in species with 34 carbons (*e.g.* PS and PA) and 36 carbons (*e.g.* PE and PA). For CL with four fatty acyl chains, the *pah1*Δ mutation caused increases (*e.g.* ~2-fold) in many of the species with 64 and 66 carbons.

Respiratory supercomplexes are major mitochondrial components for oxidative phosphorylation that transfer electrons and create a proton gradient for ATP synthesis (78). In *Saccharomyces cerevisiae*, the electron transport chain complexes III and IV associate to form the supercomplexes III_2IV (trimer) and III_2IV_2 (tetramer) (79). The phospholipid CL is essential for organization of complexes III and IV into a supercomplex in intact yeast mitochondria (58). Although the *pah1*Δ mutation did not affect the amount of CL in the mitochondria, it did result in elevated levels of unsaturated fatty acyl chains (see above). Because of this result, we examined the respiratory supercomplexes in the mitochondria of *pah1*Δ mutant cells grown in YPEG medium. The purified mitochondria were solubilized with digitonin followed by blue native-PAGE. Immunoblot analysis showed that the wild type and *pah1*Δ mutant contained the trimeric and tetrameric forms of respiratory supercomplexes, which migrated at the expected size (Fig. 5*A*). Compared with the wild type, however, the *pah1*Δ mutant exhibited a 30% reduction in the levels of the respiratory supercomplexes (Fig. 5*B*).

*Mitochondrial Oxygen Consumption, Membrane Potential, and F_1F_0-ATP Synthase Activity of the pah1*Δ *Mutant*—The *pah1*Δ mutant (3.05 ± 0.4 nmol O_2/min/$A_{600\ nm}$) showed no major difference from the wild type control (2.7 ± 0.7 nmol O_2/min/$A_{600\ nm}$) in the rate of oxygen consumption. Likewise, the mitochondrial membrane potential of the *pah1*Δ mutant (1.4 ± 0.3 arbitrary units of fluorescence) was not significantly different from that of the wild type (1.2 ± 0.2 arbitrary units of fluorescence). In oxidative phosphorylation, the production of ATP occurs by mitochondrial F_1F_0-ATP synthase coupled with the H^+ flux (80–82). The enzyme also catalyzes the reverse reaction (*i.e.* ATP hydrolysis in the absence of membrane potential or a pH gradient (83)). We measured the activity of F_1F_0-ATP synthase as its ATPase activity from the mitochondria of wild type and *pah1*Δ mutant cells. This analysis showed that the mitochondrial F_1F_0-ATPase activity of the *pah1*Δ mutant (0.55 ± 0.08 nmol/min/mg) was not significantly different from that of the wild type control (0.58 ± 0.07 nmol/min/mg). For this assay, ATP must be transported into the mitochondrial matrix for exchange with ADP (84). Thus, the level of ATPase activity exhibited by the *pah1*Δ mutant indicates that the mutation affects neither F_1F_0-ATPase nor the ATP/ADP transport function of the mitochondria.

*pah1*Δ *Mutant Exhibits a Decrease in Cellular ATP That Inversely Correlates with an Increase in Cellular Membrane Phospholipids*—The cellular levels of ATP were measured in wild type and *pah1*Δ mutant cells during growth on SC medium (Fig. 6). During the exponential phase of growth, the ATP levels of the *pah1*Δ mutant were similar to those of the wild type control. As cells progressed to the post-diauxic and stationary phases of growth, the amounts of ATP in both the wild type and *pah1*Δ mutant cells declined. However, the levels of ATP in the

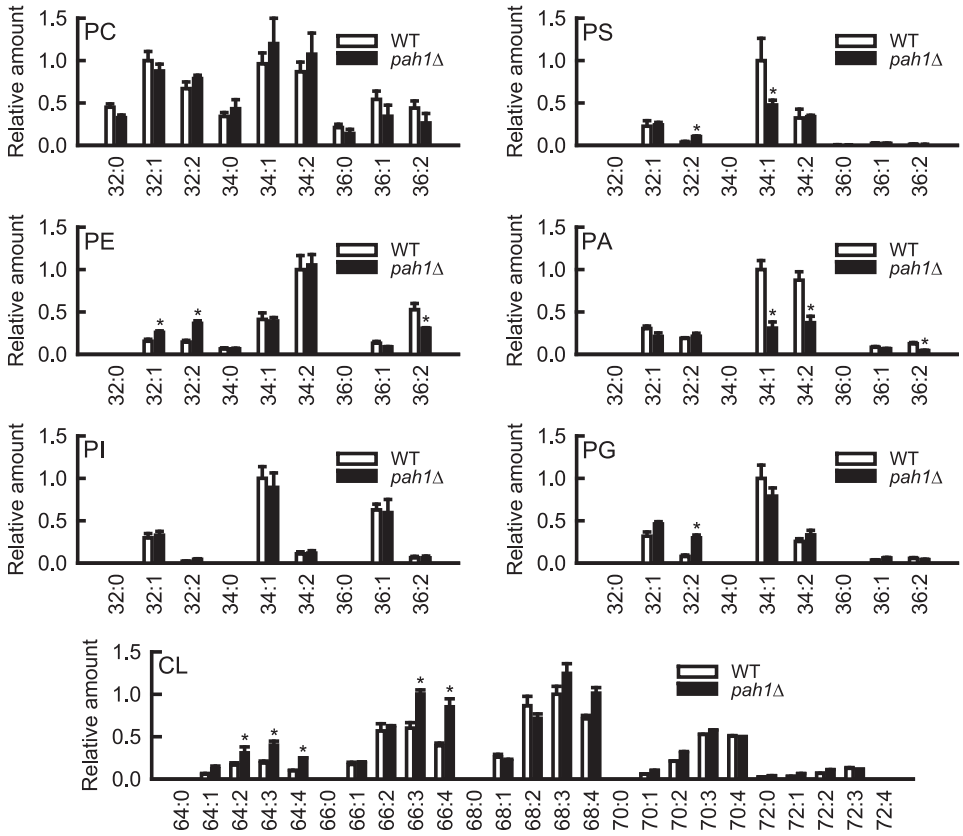

FIGURE 4. **Mitochondria of the *pah1*Δ mutant exhibit altered levels of phospholipid molecular species.** Lipids were extracted from the mitochondria of wild type and *pah1*Δ mutant cells grown to the stationary phase in SC medium and analyzed by liquid chromatography-electrospray ionization quadrupole time-of-flight mass spectrometry. For each phospholipid molecular species, the peak area of the extraction ion current of the exact *m/z* of the negative ion was determined and then normalized to that of the most abundant molecular species in each phospholipid class. The data are the averages of two separate experiments ± S.D. (*error bars*). *, $p < 0.05$ *versus* WT.

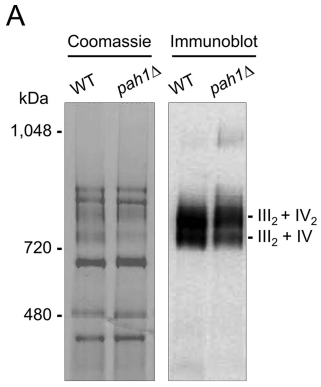

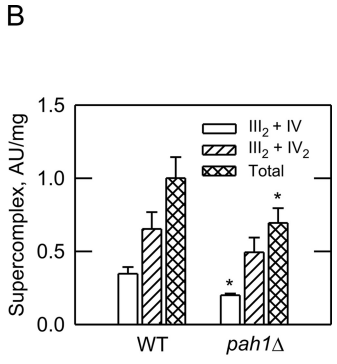

FIGURE 5. **Mitochondria of the *pah1*Δ mutant exhibit reduced levels of respiratory supercomplexes.** *A*, mitochondria from wild type and *pah1*Δ mutant cells grown in YPEG were solubilized in digitonin, and the proteins were separated by blue native-PAGE. Following the electrophoresis, the proteins were transferred to a PVDF membrane, which was then probed with antibodies raised against subunit III of complex IV. *B*, amounts of the tetramer (III_2IV_2) and trimer (III_2IV) supercomplexes were analyzed with Quantity One software. A representative Coomassie Blue-stained gel is shown in *A*, and the quantitation data shown in *B* is the average of three experiments ± S.D. (*error bars*). *, $p < 0.05$ *versus* WT. *AU*, arbitrary units.

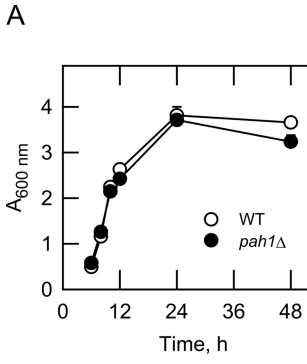

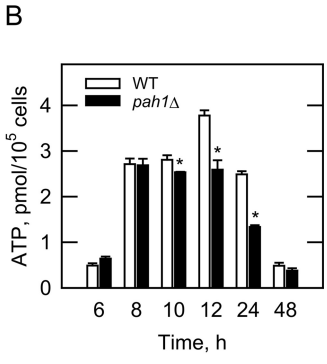

FIGURE 6. ***pah1*Δ mutant exhibits reduced levels of ATP as cells progress into the stationary phase of growth.** Wild type and *pah1*Δ mutant cells were grown in SC medium. *A*, cell densities were monitored at 600 nm. *B*, cells were harvested at the indicated time points and used for the analysis of cellular ATP. Each data point represents the average of three experiments ± S.D. (*error bars*). *, $p < 0.05$ *versus* WT.

mutant cells rapidly lowered (*e.g.* 45% at 24 h) when compared with those in the wild type control (Fig. 6*B*). At the 48-h time point, the reduced ATP levels in the *pah1*Δ mutant and wild type were not significantly different. The decreased level of ATP in the *pah1*Δ mutant correlates with 2-fold increases in the total cellular phospholipids and fatty acids when compared with wild type cells (6, 35). In a complementary experiment, we examined the levels of ATP and lipids in wild type and the *pah1*Δ mutant. Cells were grown to exponential phase in SC medium and then transferred to fresh SC medium containing glycerol as the carbon source. The shift to the glycerol-containing medium halted the growth of the *pah1*Δ mutant, consistent with the lack of growth on solid growth medium containing glycerol as the carbon source. Two and 4 h following the transfer to the glycerol-containing medium, the cellular ATP level of

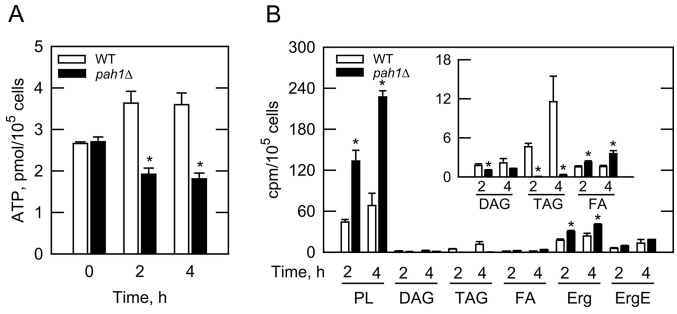

FIGURE 7. ***pah1*Δ mutant exhibits a decreased level of cellular ATP that inversely correlates with an increase in membrane phospholipids.** Wild type and *pah1*Δ mutant cells were grown to late exponential phase in SC medium. Cells were washed with sterilized distilled water and transferred to SC medium with glycerol as the carbon source. *A*, cellular ATP levels were determined from cells harvested at the indicated time intervals. *B*, cells were incubated with [2-^{14}C]acetate (1 μCi/ml) to label cellular lipids. At the indicated time points, lipids were extracted, separated by TLC, and visualized by phosphorimaging, and their amounts were analyzed with ImageQuant software using [2-^{14}C]acetate as a standard. Each data point represents the average of three experiments ± S.D. (*error bars*). *PL,* phospholipids; *FA,* fatty acids; *Erg,* ergosterol; *ErgE,* ergosterol ester. *, $p < 0.05$ *versus* WT.

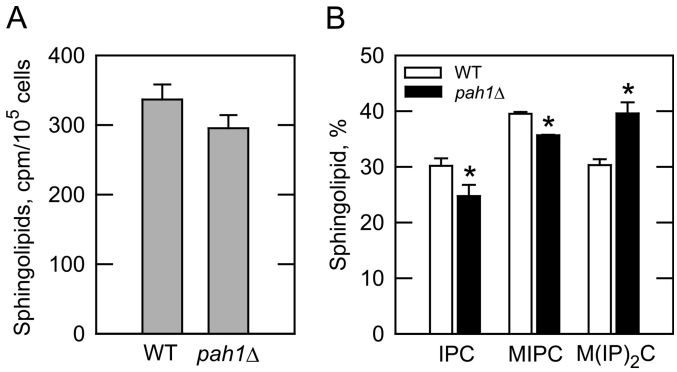

FIGURE 8. **Effect of the *pah1*Δ mutation on the composition of phosphoinositol-containing sphingolipids.** Wild type and *pah1*Δ mutant cells were grown to stationary phase in SC medium containing *myo*-[2-^{3}H]inositol (10 μCi/ml). The cellular lipids were extracted and subjected to deacylation, and the phosphoinositol-containing sphingolipids were separated by TLC. *A*, total radioactivity of the phosphoinositol-containing sphingolipids was determined by scintillation counting. *B*, inositolphosphoceramide (*IPC*), mannosylinositolphosphoceramide (*MIPC*), and mannose (inositol-P)$_2$-ceramide (*M*(*IP*)$_2$*C*) were visualized by phosphorimaging, and their amounts were analyzed with ImageQuant software. The sum of sphingolipids was set to 100%. Each data point represents the average of three experiments ± S.D. (*error bars*). *, $p < 0.05$ *versus* WT.

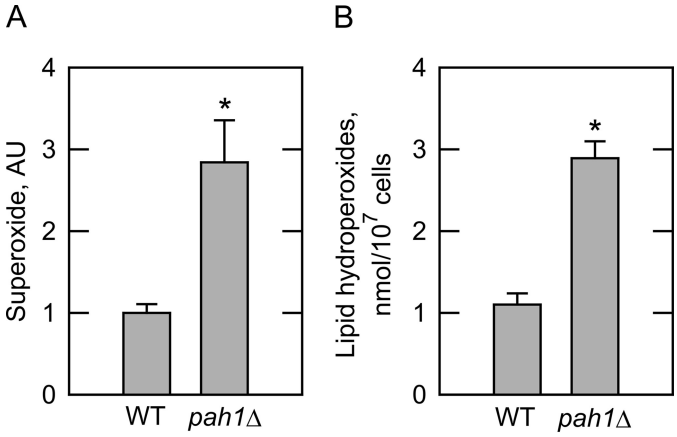

FIGURE 9. ***pah1*Δ mutant exhibits increased levels of superoxides and lipid hydroperoxides.** Wild type and *pah1*Δ mutant cells were grown to the stationary phase in SC medium. *A*, cells were washed in phosphate-buffered saline and incubated for 30 min in buffer containing MitoSOX red, and the stained cells were measured for fluorescence. *B*, lipids were extracted, and the hydroperoxides were measured with the ferric-xylenol orange complex reagent. Each data point represents the average of three experiments ± S.D. (*error bars*). *, $p < 0.05$ *versus* WT.

*pah1*Δ mutant cells was ~2-fold lower than that of the wild type control (Fig. 7*A*). The reduction of ATP levels in the *pah1*Δ mutant correlated with the time-dependent increases in cellular levels of radiolabeled phospholipids (*e.g.* 3.3-fold at 4 h) and fatty acids (*e.g.* 2.3-fold at 4 h) (Fig. 7*B*). In addition, the *pah1*Δ mutant exhibited decreases in the levels of DAG (*e.g.* 41% at 4 h) and TAG (*e.g.* 98% at 4 h) (Fig. 7*B*).

*Complex Sphingolipid Composition of the pah1*Δ *Mutant*—The *pah1*Δ mutation elevates all of the major membrane phospholipids in the stationary phase of growth (35). Among these phospholipids, PI is used as a substrate in two steps of complex sphingolipid synthesis (85, 86). Accordingly, we questioned whether sphingolipid synthesis was affected by the increased level of PI in the *pah1*Δ mutant. Wild type and *pah1*Δ mutant cells were grown to the stationary phase in the presence of *myo*-[2-^{3}H]inositol followed by lipid extraction, the deacylation of phospholipids, and the separation of the sphingolipids by TLC. The levels of complex sphingolipids in the *pah1*Δ mutant were not significantly different from those of the wild type control (Fig. 8*A*). The compositional analysis indicated that the *pah1*Δ mutation caused small decreases in the amount of inositolphosphoceramide (20%) and mannosylinositolphosphoceramide (10%) but an increase (30%) in the amount of mannose (inositol-P)$_2$-ceramide (Fig. 8*B*).

*pah1*Δ *Mutant Exhibits Increased Levels of Superoxides and Lipid Hydroperoxides, Has Reduced Levels of Superoxide Dismutase 2 and Catalase Activity, and Is Hypersensitive to Hydrogen Peroxide*—Superoxides are generated by electron leaks as by-products during oxidative phosphorylation and react readily with macromolecules (*e.g.* lipids, protein, and nucleic acids), causing detrimental effects on cellular structure and function (87–89). The reduced levels of respiratory supercomplexes in the *pah1*Δ mutant raised a question about the levels of reactive oxygen species. We examined the levels of mitochondrial superoxide in SC medium-grown stationary phase cells by staining with MitoSOX Red. This analysis showed that the superoxides in the *pah1*Δ mutant were 3-fold greater than that of the wild type control (Fig. 9*A*). Because the reactive oxygen species are known to cause oxidative damage to cellular macromolecules, we questioned whether the levels of cellular lipid hydroperoxides were affected by the *pah1*Δ mutation. The total lipid fraction was isolated from stationary phase cells grown in SC medium and were measured for hydroperoxides by a colorimetric assay using the ferrous oxidation-xylenol orange complex. This analysis showed that the cellular content of lipid hydroperoxides in the *pah1*Δ mutant was 3-fold higher than that of wild type cells (Fig. 9*B*).

Superoxide dismutase, which catalyzes the conversion of superoxide to hydrogen peroxide, was measured in SC medium-grown stationary phase cells. The mitochondrion-associated Sod2 superoxide dismutase activity was ~50% lower in the *pah1*Δ mutant when compared with the wild type control, whereas the cytosolic Sod1 activity was not significantly af-

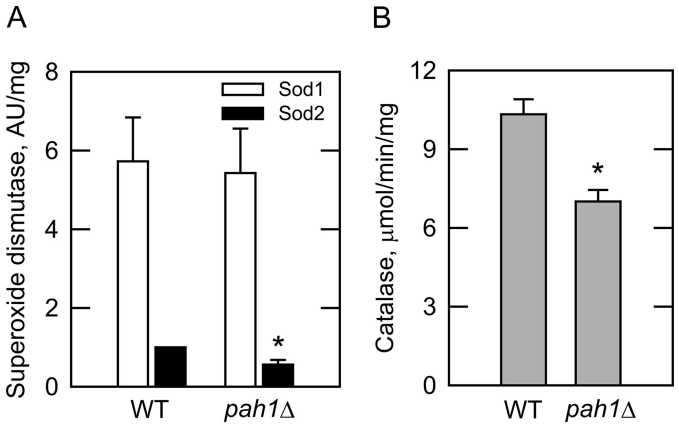

FIGURE 10. ***pah1Δ* mutant exhibits reduced superoxide dismutase and catalase activities.** Cell extracts were prepared from wild type and *pah1*Δ mutant cells grown to the stationary phase in SC medium. *A*, cell extract proteins were resolved by PAGE followed by in-gel activity staining for superoxide dismutase. The Sod1 and Sod2 forms of the enzyme were distinguished by their electrophoretic mobility. *B*, catalase activity in the cell extract was measured by following the decomposition of hydrogen peroxide at $A_{240\ nm}$. Each data point represents the average of three experiments ± S.D. (*error bars*). *, $p < 0.05$ *versus* WT.

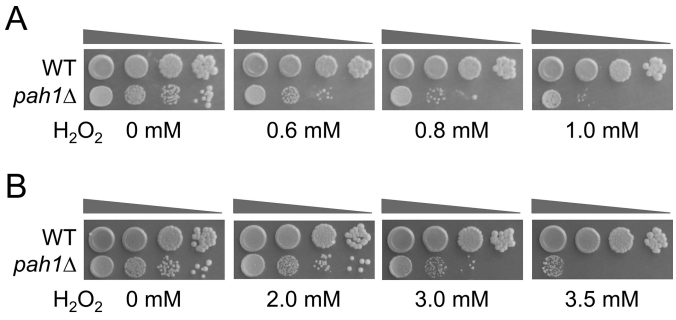

FIGURE 11. ***pah1Δ* mutant is hypersensitive to hydrogen peroxide.** Wild type and *pah1*Δ mutant cells were grown to saturation in SC (*A*) or YPD (*B*) medium. The cultures were washed and resuspended in water at $A_{600\ nm}$ = 0.67. After 10-fold serial dilutions, 5 μl of each cell suspension was spotted onto agar plates of the same growth medium containing the indicated concentrations of hydrogen peroxide (H_2O_2), followed by incubation for 3 days. The data are representative of three independent experiments.

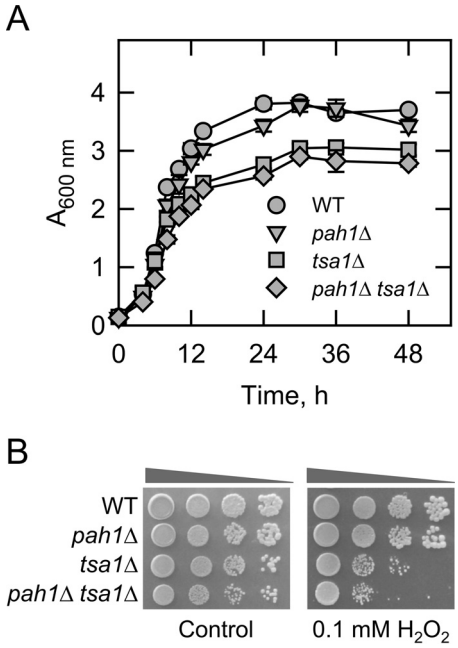

FIGURE 12. ***tsa1Δ* mutation causes a synthetic growth defect in *pah1Δ* mutant cells.** *A*, wild type, *pah1*Δ, *tsa1*Δ, and *pah1*Δ *tsa1*Δ mutant cells were grown in SC medium, and cell densities were monitored at 600 nm. *B*, indicated wild type and mutant cells were grown to saturation in SC, washed, and resuspended in water at $A_{600\ nm}$ = 0.67. After 10-fold serial dilutions, 5 μl of each cell suspension was spotted onto agar plates of the same growth medium containing 0.1 mM hydrogen peroxide (H_2O_2), followed by incubation for 3 days. The data are representative of three independent experiments.

fected in the *pah1*Δ mutant (Fig. 10*A*). The cell extract was also assayed for the activity of catalase, the enzyme that decomposes hydrogen peroxide to water and oxygen. This analysis showed that the *pah1*Δ mutant had a 32% reduction in catalase activity (Fig. 10*B*). Given these observations, we questioned whether the growth of the *pah1*Δ mutant would be affected by hydrogen peroxide. Hydrogen peroxide was added to SC or YPD media plates, and the growth of wild type and *pah1*Δ mutant cells on the growth medium was scored after 3–5 days of incubation. This analysis showed that the *pah1*Δ mutant was hypersensitive to hydrogen peroxide (Fig. 11). Higher concentrations of hydrogen peroxide were required to inhibit the growth of the mutant on rich YPD medium.

*Loss of Tsa1 Thioredoxin Peroxidase Causes a Synthetic Growth Defect with the pah1*Δ *Mutation*—Tsa1 thioredoxin peroxidase is a major antioxidant enzyme in yeast that protects cells against oxidation systems capable of generating reactive oxygen species (90, 91). The lack of *TSA1* has been shown to cause synthetic lethality with the lack of *PAH1* (92). In the genetic background examined here, the *pah1*Δ *tsa1*Δ mutant was viable when grown in SC medium (Fig. 12*A*). However, the double mutant grew to a lower cell density when compared with the *tsa1*Δ mutant, which itself grew to a lower density when compared with the *pah1*Δ mutant or the wild type control (Fig. 12*A*). We examined the effect of the *tsa1*Δ mutation on the hydrogen peroxide sensitivity of *pah1*Δ mutant cells. In this experiment, we utilized the concentration of hydrogen peroxide (*e.g.* 0.1 mM) that was not inhibitory to the *pah1*Δ mutant but was inhibitory to the *tsa1*Δ mutant (Fig. 12*B*). The *pah1*Δ mutation exacerbated the inhibitory effect of hydrogen peroxide on the growth of the *tsa1*Δ mutant (Fig. 12*B*), indicating a synthetic growth defect caused by the *pah1*Δ and *tsa1*Δ mutations.

*dgk1*Δ *Mutation Suppresses the Shortened Chronological Life Span, the Hypersensitivity to Hydrogen Peroxide, and the Growth Defect on Non-fermentable Carbon Sources of the pah1*Δ *Mutant*—We examined the effect of the *pah1*Δ mutation on the chronological life span, which is defined as the length of time that non-dividing cells survive (44). Wild type and *pah1*Δ mutant cells were grown to the stationary phase in SC medium, and then over time they were examined for their ability to form colonies on rich YPD growth medium. The wild type control lost about 50% viability 8 days after reaching quiescence (Fig. 13). In contrast, it took only 3 days for the *pah1*Δ mutant to lose the same extent of viability; no *pah1*Δ mutant cell was viable 8 days after reaching quiescence (Fig. 13).

The Dgk1 DAG kinase counterbalances the activity of Pah1 PAP by catalyzing the CTP-dependent conversion of DAG to PA (47). Several *pah1*Δ mutant phenotypes, which include an irregular nuclear/ER membrane expansion, reduced lipid droplet formation, and increased cellular phospholipid content, are

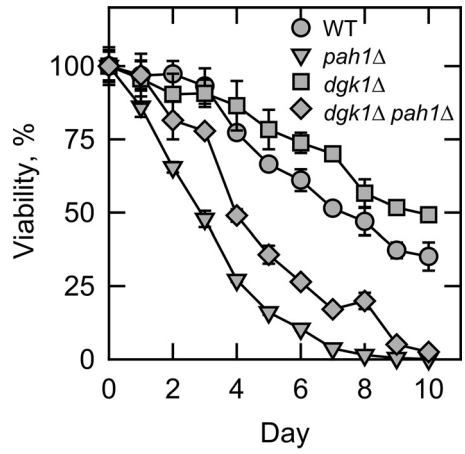

FIGURE 13. ***dgk1*Δ mutation suppresses the shortened chronological life span of the *pah1*Δ mutant.** Wild type, *pah1*Δ, *dgk1*Δ, and *dgk1*Δ *pah1*Δ mutant cells were grown in SC medium to the stationary phase. The stationary phase cultures (*day 0*) were incubated for additional 10 days during which aliquots were taken daily and plated onto YPD agar plates. The colonies formed after 2 days of incubation were scored as being derived from viable cells. The cell viability at day 0 was set at 100%. Each data point represents the average of three experiments ± S.D. (*error bars*).

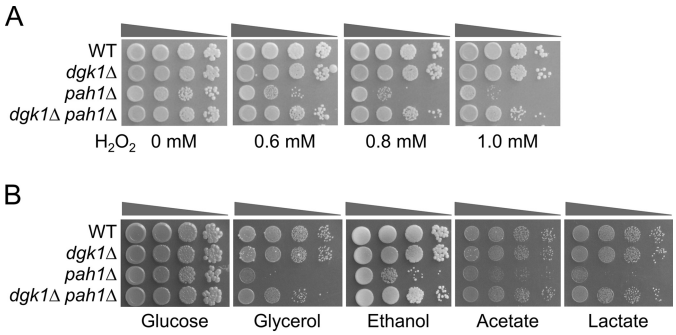

FIGURE 14. ***dgk1*Δ mutation suppresses the growth defect of the *pah1*Δ mutant in the presence of hydrogen peroxide and in culture medium containing non-fermentable carbon sources.** *A*, wild type, *pah1*Δ, *dgk1*Δ, and *dgk1*Δ *pah1*Δ mutant cells were grown to saturation in SC (*A*) or YPD (*B*) medium. The cultures were washed and resuspended in water at $A_{600\ nm}$ = 0.67. After 10-fold serial dilutions, 5 μl of each cell suspension was spotted onto agar plates of SC medium containing the indicated concentrations of hydrogen peroxide (H_2O_2) (*A*) or YP medium containing the indicated carbon sources (*B*). The cells grown on agar medium containing glucose as the carbon source were incubated for 3 days, whereas cells grown on medium with non-fermentable carbon sources were incubated for 5 days. The data shown in *A* and *B* are representative of three independent experiments.

complemented by the *dgk1*Δ mutation (35, 36, 47). We questioned whether the *dgk1*Δ mutation also suppresses some of the phenotypes described here. The *dgk1*Δ mutation extended the chronological life span of the *pah1*Δ mutant by 2 days (Fig. 13). In fact, the *dgk1*Δ mutation by itself caused an increase in chronological life span; ~50% of the culture was still viable 10 days after quiescence. The deletion of *DGK1* also complemented the growth defects of *pah1*Δ mutant cells exposed to hydrogen peroxide (Fig. 14*A*) and permitted growth of the mutant on medium with non-fermentable carbon sources (Fig. 14*B*). The *dgk1*Δ mutant itself grew on non-fermentable carbon sources and was insensitive to growth inhibition by hydrogen peroxide.

Discussion

In *S. cerevisiae*, Pah1 PAP plays a crucial role in the synthesis of the storage lipid TAG, and in the regulation of membrane phospholipid synthesis (2, 3, 12, 13). The loss of Pah1 PAP activity, which affects the levels of both its substrate PA and product DAG, results in striking changes in the composition of cellular lipids, such as a great reduction in the levels TAG, an accumulation of fatty acids, and a significant increase in membrane phospholipids (6, 11, 35). These phenotypic changes in lipid metabolism are directly or indirectly coupled to other phenotypes, such as an irregular expansion of the nuclear/ER membrane, marked vacuole fragmentation, and increased fatty acid-induced lipotoxicity (11, 29, 34, 35, 38). Similarly, in mammalian cells, loss of lipin PAP activity results in metabolic disorders that include lipodystrophy, insulin resistance, peripheral neuropathy, rhabdomyolysis, and inflammation (30, 93–101).

The initial characterization of the *pah1*Δ[4] mutant indicated a respiratory-deficient phenotype because the cells are unable to grow on glycerol as the carbon source (41). In this work, we confirmed that the *pah1*Δ mutant has a growth defect on non-fermentable carbon sources, but we could not attribute this growth defect to respiratory deficiency; the mutant did not exhibit major changes in oxygen consumption rate, membrane potential, F_1F_0-ATP synthase activity, or gross mitochondrial morphology. That the *pah1*Δ mutant is not respiratory-deficient is also indicated by the lack of a petite phenotype (41), which is typical of mutants in lipid metabolism that are respiratory-deficient (76, 102, 103).

Although mutations in PAP-encoding *PAH1* (11) and *Lpin1* (104) genes in yeast and mice, respectively, cause similar alterations in lipid metabolism, their effects on some physiological functions may differ. In contrast to the *pah1*Δ mutant, which does not exhibit a clear defect in mitochondrial morphology and function, the lipin 1-deficient mouse accumulates large, misshapen mitochondria in muscle whose disorganized cristae become evident after statin treatment. In addition, the lipin 1-deficient muscle is significantly defective in increasing oxygen consumption in response to a mitochondrial uncoupler (104). These phenotypes of lipin 1 deficiency are ascribed to a defect in mitochondrial autophagy that is activated through the DAG-dependent protein kinase D-Vps34 phosphoinositide 3-kinase signaling pathway (104).

The *pah1*Δ mutation did not have a major effect on the content of the major mitochondrial phospholipids CL and PE, which have overlapping involvements in mitochondrial functions that include oxidative phosphorylation (105). However, the mitochondrial phospholipid that was affected by the *pah1*Δ mutation was PA. This was an unexpected result because the major effect of the *pah1*Δ mutation on total cellular membrane phospholipids is an increase in PA content (11, 35). The reduction in PA does not appear to be due to its increased utilization; the mass of the mitochondrial phospholipids was not affected by the *pah1*Δ mutation. That the mitochondrial lipid mass was not affected by the *pah1*Δ mutation also differs from the effect that the mutation has on total cellular lipids whose amounts increase in mutant cells (6, 11, 35). Because PA is synthesized in the ER (3), it is unclear whether or not the reduction in PA

[4] *pah1*Δ was previously known as *smp2*Δ.

content was a consequence of a defect in ER to mitochondrial trafficking (106) or due to some other metabolic processes. In mammalian cells, the level of PA is thought to be involved in mitochondrial fusion and fission events (107, 108). An increase in PA content, as mediated by phospholipase D activity, induces mitochondrial fusion/tubulation (107), whereas the depletion of PA, as mediated by phospholipase A_1 activity, induces mitochondrial fission/fragmentation (108). Based on these observations, we speculated that the *pah1*Δ mutant with a reduced PA content in mitochondria might exhibit a fragmented mitochondrial morphology in stationary phase cells, but this is not the case as the mutant exhibits typical mitochondrial tubulation morphology.

Among the mitochondrial functions of CL is the requirement for the formation/stability of respiratory supercomplexes (58, 77). The levels of CL and its molecular species indicate that the *pah1*Δ mutant is not defective in the synthesis and remodeling of the mitochondrial phospholipid. Despite its increases in the levels of CL molecules with unsaturated fatty acyl chains, the *pah1*Δ mutant was shown to contain a reduced (30%) level of respiratory supercomplexes. In light of the recent finding that remodeling of the CL fatty acyl groups does not affect mitochondrial morphology or oxidative phosphorylation (109), it is unclear whether the changes in CL molecular species have an effect on the respiratory supercomplexes. Respiratory supercomplexes are thought to play a role in the enhancement of electron flow and thereby to prevent the formation of excess oxygen radicals (78, 110). Thus, it is possible that the reduced level of the supercomplexes in the *pah1*Δ mutant might contribute to the elevated level of superoxide.

Despite the fact that the *pah1*Δ mutant is not respiratory-deficient, it has a reduced amount of ATP. ATP is required for the synthesis of fatty acyl-CoA molecules as well as for the synthesis of CTP, the essential nucleotide required for the synthesis of phospholipids (1, 3, 111). The reduction in ATP exhibited an inverse correlation with the increase in cellular membrane phospholipid synthesis that occurs when *pah1*Δ mutant cells progress into the stationary phase (6, 11, 35). This relationship was also observed when late exponential phase glucose-grown cells were transferred to glycerol-containing growth medium. We posit that the decreased ATP content in *pah1*Δ mutant cells is the result of its overconsumption for membrane phospholipid synthesis, and as a consequence, the reduced level of ATP contributes to the growth defect on non-fermentable carbon sources and a reduced chronological life span.

To generate ATP in mitochondria, electrons are transferred to oxygen through the electron transport chain, and during this process, reactive oxygen species are produced that can cause damage to macromolecules, ultimately resulting in the loss of cell viability (68, 112–114). In this regard, we discovered that stationary phase *pah1*Δ mutant cells exhibit elevated levels of superoxide and cellular lipid hydroperoxides. Contributing factors include the reduced level of respiratory supercomplexes (see above) and the reduced activities of Sod2 superoxide dismutase and catalase that are responsible for removing reactive oxygen species. In addition, the elevated level of membrane phospholipids, which are prone to oxidation (115), provides an explanation why the *pah1*Δ mutant might be more susceptible to oxidative stress. Consequently, *pah1*Δ mutant cells were hypersensitive to hydrogen peroxide. That the *pah1*Δ mutant is more prone to oxidative stress than the wild type is further supported by the synthetic growth defect imparted by the *tsa1*Δ mutation.

Oxidative stress and accelerated aging are intimately related (110, 116, 117). Indeed, the *pah1*Δ mutant, which is prone to oxidative stress, had a significantly reduced chronological life span. The loss of Dgk1 DAG kinase in the *pah1*Δ mutant partially complemented its defect in chronological life span. That the *dgk1*Δ mutation suppresses the increased synthesis of membrane phospholipids in the *pah1*Δ mutant, but does not alleviate its defect in TAG synthesis (47), indicates that the shortened chronological life span of the *pah1*Δ mutant is due, at least in part, to the increased synthesis of membrane phospholipids. This hypothesis is further supported by the fact that the *dgk1*Δ mutation also alleviates the hypersensitivity of the *pah1*Δ mutant to hydrogen peroxide and allows for its growth on non-fermentable carbon sources.

Although the work presented here supports the notion that the overconsumption of ATP for lipid synthesis and oxidative stress contributes to reduced chronological life span, we cannot rule out other mechanisms that may come into play as a result of the altered regulation of lipid synthesis that occurs in the *pah1*Δ mutant. It is known that a defect in sphingolipid synthesis, as mediated by pharmacological inhibition or down-regulating expression of serine palmitoyltransferase (the first enzyme in the sphingolipid synthesis pathway (86)), extends chronological life span in yeast (118). This process involves the down-regulation of the Pkh1/2-Sch9 signaling pathway (118), which in turn activates the Snf1/AMP kinase signaling pathway and down-regulates the protein kinase A and target of rapamycin complex 1 signaling pathways (119). Because PI, one of the major phospholipids that is elevated in the *pah1*Δ mutant (35), is the direct precursor for the synthesis of inositolphosphoceramide and mannose (inositol-P)$_2$-ceramide (85, 86), we considered the hypothesis that the reduced chronological life span in the *pah1*Δ mutant might also be ascribed to an increase in membrane sphingolipids. However, despite its elevated PI content, the *pah1*Δ mutant did not exhibit major changes in sphingolipids. Additional studies will be required to further explore other mechanisms (*e.g.* the target of rapamycin complex 1 signaling pathway) that might be involved in controlling the chronological life span of the *pah1*Δ mutant.

In conclusion, the work reported here emphasizes the importance of Pah1 PAP in regulating the coordinate synthesis of TAG and membrane phospholipids. In particular, this work reveals a novel role of Pah1 PAP in the chronological life span that is contributed by energy expenditure and oxidative stress.

Author Contributions—Y. P. performed the experiments and prepared the manuscript. E. M. performed the analyses of mitochondrial respiratory supercomplexes and morphology by electron microscopy. T. A. G. analyzed the mitochondrial phospholipid molecular species by mass spectrometry. G. S. H. and G. M. C. directed the research and contributed to the preparation of the manuscript. All authors analyzed the results and approved the final version of the manuscript.

Acknowledgment—We thank William Dowhan for helpful discussions during the course of this work.

References

1. Chang, Y.-F., and Carman, G. M. (2008) CTP synthetase and its role in phospholipid synthesis in the yeast *Saccharomyces cerevisiae*. *Prog. Lipid Res.* **47,** 333–339
2. Carman, G. M., and Han, G.-S. (2011) Regulation of phospholipid synthesis in the yeast *Saccharomyces cerevisiae*. *Annu. Rev. Biochem.* **80,** 859–883
3. Henry, S. A., Kohlwein, S. D., and Carman, G. M. (2012) Metabolism and regulation of glycerolipids in the yeast *Saccharomyces cerevisiae*. *Genetics* **190,** 317–349
4. Taylor, F. R., and Parks, L. W. (1979) Triacylglycerol metabolism in *Saccharomyces cerevisiae* relation to phospholipid synthesis. *Biochim. Biophys. Acta* **575,** 204–214
5. Hosaka, K., and Yamashita, S. (1984) Regulatory role of phosphatidate phosphatase in triacylglycerol synthesis of *Saccharomyces cerevisiae*. *Biochim. Biophys. Acta* **796,** 110–117
6. Pascual, F., Soto-Cardalda, A., and Carman, G. M. (2013) *PAH1*-encoded phosphatidate phosphatase plays a role in the growth phase- and inositol-mediated regulation of lipid synthesis in *Saccharomyces cerevisiae*. *J. Biol. Chem.* **288,** 35781–35792
7. Kurat, C. F., Wolinski, H., Petschnigg, J., Kaluarachchi, S., Andrews, B., Natter, K., and Kohlwein, S. D. (2009) Cdk1/Cdc28-dependent activation of the major triacylglycerol lipase Tgl4 in yeast links lipolysis to cell-cycle progression. *Mol. Cell* **33,** 53–63
8. Rajakumari, S., Grillitsch, K., and Daum, G. (2008) Synthesis and turnover of non-polar lipids in yeast. *Prog. Lipid Res.* **47,** 157–171
9. Gaspar, M. L., Hofbauer, H. F., Kohlwein, S. D., and Henry, S. A. (2011) Coordination of storage lipid synthesis and membrane biogenesis: evidence for cross-talk between triacylglycerol metabolism and phosphatidylinositol synthesis. *J. Biol. Chem.* **286,** 1696–1708
10. Fakas, S., Konstantinou, C., and Carman, G. M. (2011) *DGK1*-encoded diacylglycerol kinase activity is required for phospholipid synthesis during growth resumption from stationary phase in *Saccharomyces cerevisiae*. *J. Biol. Chem.* **286,** 1464–1474
11. Han, G.-S., Wu, W.-I., and Carman, G. M. (2006) The *Saccharomyces cerevisiae* lipin homolog is a Mg^{2+}-dependent phosphatidate phosphatase enzyme. *J. Biol. Chem.* **281,** 9210–9218
12. Carman, G. M., and Han, G.-S. (2006) Roles of phosphatidate phosphatase enzymes in lipid metabolism. *Trends Biochem. Sci.* **31,** 694–699
13. Carman, G. M., and Han, G.-S. (2009) Phosphatidic acid phosphatase, a key enzyme in the regulation of lipid synthesis. *J. Biol. Chem.* **284,** 2593–2597
14. Pascual, F., and Carman, G. M. (2013) Phosphatidate phosphatase, a key regulator of lipid homeostasis. *Biochim. Biophys. Acta* **1831,** 514–522
15. Soto-Cardalda, A., Fakas, S., Pascual, F., Choi, H. S., and Carman, G. M. (2012) Phosphatidate phosphatase plays role in zinc-mediated regulation of phospholipid synthesis in yeast. *J. Biol. Chem.* **287,** 968–977
16. Wu, W.-I., Lin, Y.-P., Wang, E., Merrill, A. H., Jr., and Carman, G. M. (1993) Regulation of phosphatidate phosphatase activity from the yeast *Saccharomyces cerevisiae* by sphingoid bases. *J. Biol. Chem.* **268,** 13830–13837
17. Wu, W.-I., and Carman, G. M. (1996) Regulation of phosphatidate phosphatase activity from the yeast *Saccharomyces cerevisiae* by phospholipids. *Biochemistry* **35,** 3790–3796
18. Wu, W.-I., and Carman, G. M. (1994) Regulation of phosphatidate phosphatase activity from the yeast *Saccharomyces cerevisiae* by nucleotides. *J. Biol. Chem.* **269,** 29495–29501
19. O'Hara, L., Han, G.-S., Peak-Chew, S., Grimsey, N., Carman, G. M., and Siniossoglou, S. (2006) Control of phospholipid synthesis by phosphorylation of the yeast lipin Pah1p/Smp2p Mg^{2+}-dependent phosphatidate phosphatase. *J. Biol. Chem.* **281,** 34537–34548
20. Choi, H.-S., Su, W.-M., Han, G.-S., Plote, D., Xu, Z., and Carman, G. M. (2012) Pho85p-Pho80p phosphorylation of yeast Pah1p phosphatidate phosphatase regulates its activity, location, abundance, and function in lipid metabolism. *J. Biol. Chem.* **287,** 11290–11301
21. Su, W.-M., Han, G.-S., Casciano, J., and Carman, G. M. (2012) Protein kinase A-mediated phosphorylation of Pah1p phosphatidate phosphatase functions in conjunction with the Pho85p-Pho80p and Cdc28p-cyclin B kinases to regulate lipid synthesis in yeast. *J. Biol. Chem.* **287,** 33364–33376
22. Su, W.-M., Han, G.-S., and Carman, G. M. (2014) Yeast Nem1-Spo7 protein phosphatase activity on Pah1 phosphatidate phosphatase is specific for the Pho85-Pho80 protein kinase phosphorylation sites. *J. Biol. Chem.* **289,** 34699–34708
23. Choi, H.-S., Su, W.-M., Morgan, J. M., Han, G.-S., Xu, Z., Karanasios, E., Siniossoglou, S., and Carman, G. M. (2011) Phosphorylation of phosphatidate phosphatase regulates its membrane association and physiological functions in *Saccharomyces cerevisiae:* identification of Ser^{602}, Thr^{723}, and Ser^{744} as the sites phosphorylated by *CDC28* (*CDK1*)-encoded cyclin-dependent kinase. *J. Biol. Chem.* **286,** 1486–1498
24. Xu, Z., Su, W.-M., and Carman, G. M. (2012) Fluorescence spectroscopy measures yeast *PAH1*-encoded phosphatidate phosphatase interaction with liposome membranes. *J. Lipid Res.* **53,** 522–528
25. Karanasios, E., Han, G.-S., Xu, Z., Carman, G. M., and Siniossoglou, S. (2010) A phosphorylation-regulated amphipathic helix controls the membrane translocation and function of the yeast phosphatidate phosphatase. *Proc. Natl. Acad. Sci. U.S.A.* **107,** 17539–17544
26. Su, W. M., Han, G. S., and Carman, G. M. (2014) Cross-talk phosphorylations by protein kinase C and Pho85p-Pho80p protein kinase regulate Pah1p phosphatidate phosphatase abundance in *Saccharomyces cerevisiae*. *J. Biol. Chem.* **289,** 18818–18830
27. Pascual, F., Hsieh, L.-S., Soto-Cardalda, A., and Carman, G. M. (2014) Yeast Pah1p phosphatidate phosphatase is regulated by proteasome-mediated degradation. *J. Biol. Chem.* **289,** 9811–9822
28. Hsieh, L.-S., Su, W.-M., Han, G.-S., and Carman, G. M. (2015) Phosphorylation regulates the ubiquitin-independent degradation of yeast Pah1 phosphatidate phosphatase by the 20S proteasome. *J. Biol. Chem.* **290,** 11467–11478
29. Han, G.-S., Siniossoglou, S., and Carman, G. M. (2007) The cellular functions of the yeast lipin homolog Pah1p are dependent on its phosphatidate phosphatase activity. *J. Biol. Chem.* **282,** 37026–37035
30. Péterfy, M., Phan, J., Xu, P., and Reue, K. (2001) Lipodystrophy in the *fld* mouse results from mutation of a new gene encoding a nuclear protein, lipin. *Nat. Genet.* **27,** 121–124
31. Reue, K., and Brindley, D. N. (2008) Multiple roles for lipins/phosphatidate phosphatase enzymes in lipid metabolism. *J. Lipid Res.* **49,** 2493–2503
32. Reue, K., and Dwyer, J. R. (2009) Lipin proteins and metabolic homeostasis. *J. Lipid Res.* **50,** S109–S114
33. Csaki, L. S., Dwyer, J. R., Fong, L. G., Tontonoz, P., Young, S. G., and Reue, K. (2013) Lipins, lipinopathies, and the modulation of cellular lipid storage and signaling. *Prog. Lipid Res.* **52,** 305–316
34. Santos-Rosa, H., Leung, J., Grimsey, N., Peak-Chew, S., and Siniossoglou, S. (2005) The yeast lipin Smp2 couples phospholipid biosynthesis to nuclear membrane growth. *EMBO J.* **24,** 1931–1941
35. Fakas, S., Qiu, Y., Dixon, J. L., Han, G.-S., Ruggles, K. V., Garbarino, J., Sturley, S. L., and Carman, G. M. (2011) Phosphatidate phosphatase activity plays a key role in protection against fatty acid-induced toxicity in yeast. *J. Biol. Chem.* **286,** 29074–29085
36. Adeyo, O., Horn, P. J., Lee, S., Binns, D. D., Chandrahas, A., Chapman, K. D., and Goodman, J. M. (2011) The yeast lipin orthologue Pah1p is important for biogenesis of lipid droplets. *J. Cell Biol.* **192,** 1043–1055
37. Carman, G. M., and Henry, S. A. (2007) Phosphatidic acid plays a central role in the transcriptional regulation of glycerophospholipid synthesis in *Saccharomyces cerevisiae*. *J. Biol. Chem.* **282,** 37293–37297
38. Sasser, T., Qiu, Q. S., Karunakaran, S., Padolina, M., Reyes, A., Flood, B., Smith, S., Gonzales, C., and Fratti, R. A. (2012) The yeast lipin 1 orthologue Pah1p regulates vacuole homeostasis and membrane fusion. *J. Biol. Chem.* **287,** 2221–2236
39. Lussier, M., White, A. M., Sheraton, J., di Paolo, T., Treadwell, J., Southard, S. B., Horenstein, C. I., Chen-Weiner, J., Ram, A. F., Kapteyn, J. C.,

Roemer, T. W., Vo, D. H., Bondoc, D. C., Hall, J., Zhong, W. W., *et al.* (1997) Large scale identification of genes involved in cell surface biosynthesis and architecture in *Saccharomyces cerevisiae*. *Genetics* **147,** 435–450
40. Ruiz, C., Cid, V. J., Lussier, M., Molina, M., and Nombela, C. (1999) A large-scale sonication assay for cell wall mutant analysis in yeast. *Yeast* **15,** 1001–1008
41. Irie, K., Takase, M., Araki, H., and Oshima, Y. (1993) A gene, SMP2, involved in plasmid maintenance and respiration in *Saccharomyces cerevisiae* encodes a highly charged protein. *Mol. Gen. Genet.* **236,** 283–288
42. Sambrook, J., Fritsch, E. F., and Maniatis, T. (1989) *Molecular Cloning: A Laboratory Manual*, 2nd Ed., Cold Spring Harbor Laboratory, Cold Spring Harbor, NY
43. Rose, M. D., Winston, F., and Heiter, P. (1990) *Methods in Yeast Genetics: A Laboratory Course Manual*, Cold Spring Harbor Laboratory Press, Cold Spring Harbor, NY
44. Parrella, E., and Longo, V. D. (2008) The chronological life span of *Saccharomyces cerevisiae* to study mitochondrial dysfunction and disease. *Methods* **46,** 256–262
45. Ito, H., Fukuda, Y., Murata, K., and Kimura, A. (1983) Transformation of intact yeast cells treated with alkali cations. *J. Bacteriol.* **153,** 163–168
46. Rothstein, R. (1991) Targeting, disruption, replacement, and allele rescue: integrative DNA transformation in yeast. *Methods Enzymol.* **194,** 281–301
47. Han, G.-S., O'Hara, L., Carman, G. M., and Siniossoglou, S. (2008) An unconventional diacylglycerol kinase that regulates phospholipid synthesis and nuclear membrane growth. *J. Biol. Chem.* **283,** 20433–20442
48. Carman, G. M., and Lin, Y.-P. (1991) Phosphatidate phosphatase from yeast. *Methods Enzymol.* **197,** 548–553
49. Bradford, M. M. (1976) A rapid and sensitive method for the quantitation of microgram quantities of protein utilizing the principle of protein-dye binding. *Anal. Biochem.* **72,** 248–254
50. Meisinger, C., Pfanner, N., and Truscott, K. N. (2006) Isolation of yeast mitochondria. *Methods Mol. Biol.* **313,** 33–39
51. Choi, H.-S., Han, G.-S., and Carman, G. M. (2010) Phosphorylation of yeast phosphatidylserine synthase by protein kinase A: identification of Ser^{46} and Ser^{47} as major sites of phosphorylation. *J. Biol. Chem.* **285,** 11526–11536
52. Bozzola, J. J., and Russell, L. D. (1999) *Electron Microscopy: Principles and Techniques for Biologists*, 2nd Ed., Jones and Bartlett Publisher, Boston
53. Westermann, B., and Neupert, W. (2000) Mitochondria-targeted green fluorescent proteins: convenient tools for the study of organelle biogenesis in *Saccharomyces cerevisiae*. *Yeast* **16,** 1421–1427
54. Laemmli, U. K. (1970) Cleavage of structural proteins during the assembly of the head of bacteriophage T4. *Nature* **227,** 680–685
55. Burnette, W. (1981) Western blotting: electrophoretic transfer of proteins from sodium dodecyl sulfate-polyacrylamide gels to unmodified nitrocellulose and radiographic detection with antibody and radioiodinated protein A. *Anal. Biochem.* **112,** 195–203
56. Haid, A., and Suissa, M. (1983) Immunochemical identification of membrane proteins after sodium dodecyl sulfate-polyacrylamide gel electrophoresis. *Methods Enzymol.* **96,** 192–205
57. Schägger, H., and von Jagow, G. (1991) Blue native electrophoresis for isolation of membrane protein complexes in enzymatically active form. *Anal. Biochem.* **199,** 223–231
58. Zhang, M., Mileykovskaya, E., and Dowhan, W. (2005) Cardiolipin is essential for organization of complexes III and IV into a supercomplex in intact yeast mitochondria. *J. Biol. Chem.* **280,** 29403–29408
59. Bligh, E. G., and Dyer, W. J. (1959) A rapid method of total lipid extraction and purification. *Can. J. Biochem. Physiol.* **37,** 911–917
60. Han, G.-S., Johnston, C. N., and Carman, G. M. (2004) Vacuole membrane topography of the *DPP1*-encoded diacylglycerol pyrophosphate phosphatase catalytic site from *Saccharomyces cerevisiae*. *J. Biol. Chem.* **279,** 5338–5345
61. Skipski, V. P. (1975) Thin-layer chromatography of neutral glycosphingolipids. *Methods Enzymol.* **35,** 396–425
62. Garrett, T. A., Raetz, C. R., Richardson, T., Kordestani, R., Son, J. D., and Rose, R. L. (2009) Identification of phosphatidylserylglutamate: a novel minor lipid in *Escherichia coli*. *J. Lipid Res.* **50,** 1589–1599
63. Bulat, E., and Garrett, T. A. (2011) Putative *N*-acylphosphatidylethanolamine synthase from *Arabidopsis thaliana* is a lysoglycerophospholipid acyltransferase. *J. Biol. Chem.* **286,** 33819–33831
64. Henderson, R. J., and Tocher, D. R. (1992) in *Lipid Analysis* (Hamilton, R. J., and Hamilton, S., eds) pp. 65–111, IRL Press, New York
65. Angus, W. W., and Lester, R. L. (1972) Turnover of inositol and phosphorus containing lipids in *Saccharomyces cerevisiae*: extracellular accumulation of glycerophosphorylinositol derived from phosphatidylinositol. *Arch. Biochem. Biophys.* **151,** 483–495
66. Hanson, B. A., and Lester, R. L. (1980) The extraction of inositol-containing phospholipids and phosphatidylcholine from *Saccharomyces cerevisiae* and *Neurospora crassa*. *J. Lipid Res.* **21,** 309–315
67. Jesch, S. A., Gaspar, M. L., Stefan, C. J., Aregullin, M. A., and Henry, S. A. (2010) Interruption of inositol sphingolipid synthesis triggers Stt4p-dependent protein kinase C signaling. *J. Biol. Chem.* **285,** 41947–41960
68. Bonawitz, N. D., Rodeheffer, M. S., and Shadel, G. S. (2006) Defective mitochondrial gene expression results in reactive oxygen species-mediated inhibition of respiration and reduction of yeast life span. *Mol. Cell. Biol.* **26,** 4818–4829
69. Jiang, Z. Y., Hunt, J. V., and Wolff, S. P. (1992) Ferrous ion oxidation in the presence of xylenol orange for detection of lipid hydroperoxide in low density lipoprotein. *Anal. Biochem.* **202,** 384–389
70. Somlo, M. (1968) Induction and repression of mitochondrial ATPase in yeast. *Eur. J. Biochem.* **5,** 276–284
71. Arnold, I., Pfeiffer, K., Neupert, W., Stuart, R. A., and Schägger, H. (1999) ATP synthase of yeast mitochondria. Isolation of subunit j and disruption of the *ATP18* gene. *J. Biol. Chem.* **274,** 36–40
72. Beauchamp, C., and Fridovich, I. (1971) Superoxide dismutase: improved assays and an assay applicable to acrylamide gels. *Anal. Biochem.* **44,** 276–287
73. Goldsteins, G., Keksa-Goldsteine, V., Ahtoniemi, T., Jaronen, M., Arens, E., Akerman, K., Chan, P. H., and Koistinaho, J. (2008) Deleterious role of superoxide dismutase in the mitochondrial intermembrane space. *J. Biol. Chem.* **283,** 8446–8452
74. Beers, R. F., Jr., and Sizer, I. W. (1952) A spectrophotometric method for measuring the breakdown of hydrogen peroxide by catalase. *J. Biol. Chem.* **195,** 133–140
75. Joshi, A. S., Zhou, J., Gohil, V. M., Chen, S., and Greenberg, M. L. (2009) Cellular functions of cardiolipin in yeast. *Biochim. Biophys. Acta* **1793,** 212–218
76. Zhong, Q., Gohil, V. M., Ma, L., and Greenberg, M. L. (2004) Absence of cardiolipin results in temperature sensitivity, respiratory defects, and mitochondrial DNA instability independent of *pet56*. *J. Biol. Chem.* **279,** 32294–32300
77. Pfeiffer, K., Gohil, V., Stuart, R. A., Hunte, C., Brandt, U., Greenberg, M. L., and Schägger, H. (2003) Cardiolipin stabilizes respiratory chain supercomplexes. *J. Biol. Chem.* **278,** 52873–52880
78. Saraste, M. (1999) Oxidative phosphorylation at the fin de siecle. *Science* **283,** 1488–1493
79. Schägger, H., and Pfeiffer, K. (2000) Supercomplexes in the respiratory chains of yeast and mammalian mitochondria. *EMBO J.* **19,** 1777–1783
80. Kagawa, Y., and Racker, E. (1966) Partial resolution of the enzymes catalyzing oxidative phosphorylation. X. Correlation of morphology and function in submitochondrial particles. *J. Biol. Chem.* **241,** 2475–2482
81. Macino, G., and Tzagoloff, A. (1979) Assembly of the mitochondrial membrane system: the DNA sequence of a mitochondrial ATPase gene in *Saccharomyces cerevisiae*. *J. Biol. Chem.* **254,** 4617–4623
82. Todd, R. D., Griesenbeck, T. A., and Douglas, M. G. (1980) The yeast mitochondrial adenosine triphosphatase complex: subunit stoichiometry and physical characterization. *J. Biol. Chem.* **255,** 5461–5467
83. Pullman, M. E., Penefsky, H. S., Datta, A., and Racker, E. (1960) Partial resolution of the enzymes catalyzing oxidative phosphorylation. I. Purification and properties of soluble dinitrophenol-stimulated adenosine triphosphatase. *J. Biol. Chem.* **235,** 3322–3329
84. Klingenberg, M. (2008) The ADP and ATP transport in mitochondria and its carrier. *Biochim. Biophys. Acta* **1778,** 1978–2021

85. Becker, G. W., and Lester, R. L. (1980) Biosynthesis of phosphoinositol-containing sphingolipids from phosphatidylinositol by a membrane preparation from *Saccharomyces cerevisiae*. *J. Bacteriol.* **142,** 747–754
86. Dickson, R. C. (2008) New insights into sphingolipid metabolism and function in budding yeast. *J. Lipid Res.* **49,** 909–921
87. Balaban, R. S., Nemoto, S., and Finkel, T. (2005) Mitochondria, oxidants, and aging. *Cell* **120,** 483–495
88. Fridovich, I. (1978) The biology of oxygen radicals. *Science* **201,** 875–880
89. Jamieson, D. J. (1998) Oxidative stress responses of the yeast *Saccharomyces cerevisiae*. *Yeast* **14,** 1511–1527
90. Chae, H. Z., Kim, I. H., Kim, K., and Rhee, S. G. (1993) Cloning, sequencing, and mutation of thiol-specific antioxidant gene of *Saccharomyces cerevisiae*. *J. Biol. Chem.* **268,** 16815–16821
91. Chae, H. Z., Chung, S. J., and Rhee, S. G. (1994) Thioredoxin-dependent peroxide reductase from yeast. *J. Biol. Chem.* **269,** 27670–27678
92. Pan, X., Ye, P., Yuan, D. S., Wang, X., Bader, J. S., and Boeke, J. D. (2006) A DNA integrity network in the yeast *Saccharomyces cerevisiae*. *Cell* **124,** 1069–1081
93. Phan, J., and Reue, K. (2005) Lipin, a lipodystrophy and obesity gene. *Cell Metab.* **1,** 73–83
94. Lindegaard, B., Larsen, L. F., Hansen, A. B., Gerstoft, J., Pedersen, B. K., and Reue, K. (2007) Adipose tissue lipin expression levels distinguish HIV patients with and without lipodystrophy. *Int. J. Obes.* **31,** 449–456
95. Nadra, K., de Preux Charles, A.-S., Médard, J.-J., Hendriks, W. T., Han, G.-S., Grès, S., Carman, G. M., Saulnier-Blache, J.-S., Verheijen, M. H., and Chrast, R. (2008) Phosphatidic acid mediates demyelination in *Lpin1* mutant mice. *Genes Dev.* **22,** 1647–1661
96. Zeharia, A., Shaag, A., Houtkooper, R. H., Hindi, T., de Lonlay, P., Erez, G., Hubert, L., Saada, A., de Keyzer, Y., Eshel, G., Vaz, F. M., Pines, O., and Elpeleg, O. (2008) Mutations in *LPIN1* cause recurrent acute myoglobinuria in childhood. *Am. J. Hum. Genet.* **83,** 489–494
97. Donkor, J., Zhang, P., Wong, S., O'Loughlin, L., Dewald, J., Kok, B. P., Brindley, D. N., and Reue, K. (2009) A conserved serine residue is required for the phosphatidate phosphatase activity but not transcriptional coactivator functions of lipin-1 and lipin-2. *J. Biol. Chem.* **284,** 29968–29978
98. Kim, H. B., Kumar, A., Wang, L., Liu, G. H., Keller, S. R., Lawrence, J. C., Jr., Finck, B. N., and Harris, T. E. (2010) Lipin 1 represses NFATc4 transcriptional activity in adipocytes to inhibit secretion of inflammatory factors. *Mol. Cell. Biol.* **30,** 3126–3139
99. Mul, J. D., Nadra, K., Jagalur, N. B., Nijman, I. J., Toonen, P. W., Médard, J. J., Grès, S., de Bruin, A., Han, G.-S., Brouwers, J. F., Carman, G. M., Saulnier-Blache, J. S., Meijer, D., Chrast, R., and Cuppen, E. (2011) A hypomorphic mutation in *Lpin1* induces progressively improving neuropathy and lipodystrophy in the rat. *J. Biol. Chem.* **286,** 26781–26793
100. Nadra, K., Médard, J. J., Mul, J. D., Han, G.-S., Grès, S., Pende, M., Metzger, D., Chambon, P., Cuppen, E., Saulnier-Blache, J. S., Carman, G. M., Desvergne, B., and Chrast, R. (2012) Cell autonomous lipin 1 function is essential for development and maintenance of white and brown adipose tissue. *Mol. Cell. Biol.* **32,** 4794–4810
101. Michot, C., Mamoune, A., Vamecq, J., Viou, M. T., Hsieh, L.-S., Testet, E., Lainé, J., Hubert, L., Dessein, A. F., Fontaine, M., Ottolenghi, C., Fouillen, L., Nadra, K., Blanc, E., Bastin, J., *et al.* (2013) Combination of lipid metabolism alterations and their sensitivity to inflammatory cytokines in human lipin-1-deficient myoblasts. *Biochim. Biophys. Acta* **1832,** 2103–2114
102. Henry, S. A. (1973) Death resulting from fatty acid starvation in yeast. *J. Bacteriol.* **116,** 1293–1303
103. Atkinson, K. D., Jensen, B., Kolat, A. I., Storm, E. M., Henry, S. A., and Fogel, S. (1980) Yeast mutants auxotropic for choline or ethanolamine. *J. Bacteriol.* **141,** 558–564
104. Zhang, P., Verity, M. A., and Reue, K. (2014) Lipin-1 regulates autophagy clearance and intersects with statin drug effects in skeletal muscle. *Cell Metab.* **20,** 267–279
105. Gohil, V. M., Thompson, M. N., and Greenberg, M. L. (2005) Synthetic lethal interaction of the mitochondrial phosphatidylethanolamine and cardiolipin biosynthetic pathways in *Saccharomyces cerevisiae*. *J. Biol. Chem.* **280,** 35410–35416
106. Connerth, M., Tatsuta, T., Haag, M., Klecker, T., Westermann, B., and Langer, T. (2012) Intramitochondrial transport of phosphatidic acid in yeast by a lipid transfer protein. *Science* **338,** 815–818
107. Huang, H., Gao, Q., Peng, X., Choi, S. Y., Sarma, K., Ren, H., Morris, A. J., and Frohman, M. A. (2011) piRNA-associated germline nuage formation and spermatogenesis require MitoPLD profusogenic mitochondrial-surface lipid signaling. *Dev. Cell* **20,** 376–387
108. Baba, T., Kashiwagi, Y., Arimitsu, N., Kogure, T., Edo, A., Maruyama, T., Nakao, K., Nakanishi, H., Kinoshita, M., Frohman, M. A., Yamamoto, A., and Tani, K. (2014) Phosphatidic acid (PA)-preferring phospholipase A1 regulates mitochondrial dynamics. *J. Biol. Chem.* **289,** 11497–11511
109. Baile, M. G., Sathappa, M., Lu, Y. W., Pryce, E., Whited, K., McCaffery, J. M., Han, X., Alder, N. N., and Claypool, S. M. (2014) Unremodeled and remodeled cardiolipin are functionally indistinguishable in yeast. *J. Biol. Chem.* **289,** 1768–1778
110. Genova, M. L., and Lenaz, G. (2015) The interplay between respiratory supercomplexes and ROS in aging. *Antioxid. Redox Signal.* **23,** 208–238
111. Natter, K., and Kohlwein, S. D. (2013) Yeast and cancer cells–common principles in lipid metabolism. *Biochim. Biophys. Acta* **1831,** 314–326
112. Boveris, A., Oshino, N., and Chance, B. (1972) The cellular production of hydrogen peroxide. *Biochem. J.* **128,** 617–630
113. Finkel, T., and Holbrook, N. J. (2000) Oxidants, oxidative stress and the biology of ageing. *Nature* **408,** 239–247
114. Feng, J., Bussière, F., and Hekimi, S. (2001) Mitochondrial electron transport is a key determinant of life span in *Caenorhabditis elegans*. *Dev. Cell* **1,** 633–644
115. Niki, E., Yamamoto, Y., Komuro, E., and Sato, K. (1991) Membrane damage due to lipid oxidation. *Am. J. Clin. Nutr.* **53,** 201S-205S
116. Beckman, K. B., and Ames, B. N. (1998) The free radical theory of aging matures. *Physiol. Rev.* **78,** 547–581
117. Longo, V. D., Liou, L. L., Valentine, J. S., and Gralla, E. B. (1999) Mitochondrial superoxide decreases yeast survival in stationary phase. *Arch. Biochem. Biophys.* **365,** 131–142
118. Huang, X., Liu, J., and Dickson, R. C. (2012) Down-regulating sphingolipid synthesis increases yeast lifespan. *PLoS Genet.* **8,** e1002493
119. Liu, J., Huang, X., Withers, B. R., Blalock, E., Liu, K., and Dickson, R. C. (2013) Reducing sphingolipid synthesis orchestrates global changes to extend yeast lifespan. *Aging Cell* **12,** 833–841
120. Thomas, B. J., and Rothstein, R. (1989) Elevated recombination rates in transcriptionally active DNA. *Cell* **56,** 619–630